

A simplified model of propagation and dissipation of excitation fronts

V. N. Biktashev^{1,2}

Online since 2002/11/18

¹ *Department of Mathematical Sciences, University of Liverpool, Liverpool L69 7ZL, UK*

² *On leave from: Institute for Mathematical Problems in Biology, Pushchino, 142290, Russia*

Highlighted: errors in the printed version

Abstract

An excitation wave in nerve or cardiac tissue may fail to propagate if the temporal gradient of the transmembrane voltage at the front becomes too small to excite the tissue ahead of it. A simplified mathematical model is suggested, that reproduces this phenomenon and has exact travelling front solutions. The spectrum of possible propagation speeds is bounded from below. This causes a front to dissipate if it is not allowed to propagate quickly enough. A crucial role is played by the Na inactivation gates, even if their dynamics are by an order of magnitude slower than the dynamics of the voltage.

1 Introduction.

The last decades have seen an exponential explosion in the quantitative electrophysiology of cardiac cells and detailed mathematical models of propagation of excitation in heart. These mathematical models are rather complicated and mostly studied numerically. The disadvantages of purely numerical simulations are well known: limited insight into the mechanisms of the studied phenomena, and generally unknown dependence on the numerous parameters of the models, not all of which are known equally reliably. Thus, whatever the development of the detailed models, simplified, caricature-type models that allow some degree of analytical treatment are always in great demand. The suitability of such a simplified model to a particular purpose depends, of course, on the phenomena under investigation and how the model captures their essential features; thus different simplified models can be adequate for different phenomena.

The most popular simplified model of excitable media is the FitzHugh-Nagumo (FHN) system (FitzHugh 1961, Nagumo, Arimoto & Yoshizawa 1962):

$$\begin{aligned}\frac{\partial E}{\partial t} &= D \frac{\partial^2 E}{\partial x^2} + \epsilon_E (E - E^3/3 - v), \\ \frac{\partial v}{\partial t} &= \epsilon_v (E + \beta - \gamma v).\end{aligned}\tag{1}$$

originally proposed as a simplified analogue of the Hodgkin & Huxley (1952) system of equations that gave the first complete and quantitative description of the electric action of a biological excitable system, the giant squid axon. In (1), E corresponds to the transmembrane voltage and v represents all other, slow variables. FitzHugh has shown that an appropriate 2-dimensional projection of the “phase portrait” of the point system of the Hodgkin & Huxley (HH) model looks “similar” to that of (1), and Nagumo et al. have demonstrated that it describes propagating pulses similar to those in HH. This system is much simpler than the HH model and its descendants, and allows a great deal of analytical and qualitative study, especially in the asymptotics $\epsilon_v/\epsilon_E \rightarrow +0$. Note that FHN system (1) was *not* in any way derived from the HH system. Although it is possible,

under certain rather arbitrary assumptions, to reduce point (spatially independent) HH model to a system of two ordinary differential equations “resembling” FHN (Krinsky & Kokoz 1973), the asymptotic structure, i.e. dependence on the small parameters, is then very different from the FHN system (1).

Throughout the last forty years, the FitzHugh-Nagumo system and its numerous modifications have served well as very simple but qualitatively reasonable models of the complicated processes of excitation and propagation in nerve fibre, heart muscle and other biological spatially-extended excitable systems. It appears, however, that while successfully describing successful propagation of excitation, FHN-type systems fail to adequately describe propagation failure. Yet it is propagation failure that is most important for many applications of these models, e.g. in relation with onset and persistence of fibrillation of heart muscle and sudden cardiac death. As an example of a recent study, oriented to a clinical audience, see (Weiss, Chen, Qu, Karagueuzian & Garfinkel 2000), which argues that the question of “what causes ventricular fibrillation” in fact reduces to the question of “what causes wavebreak”.

In this paper we discuss a particular mechanism of the block of excitation wave propagation, which we call dissipation of the excitation waves. We show that this mechanism is typical for realistic excitation propagation models but can not be adequately reproduced in any FHN-type system. This type of propagation failure is characterised by a loss of the sharp gradient characteristic of the normal excitation front, followed by purely diffusive spread of the voltage. This is in contrast with the failure of propagation in FHN-type systems, in which the structured front persists, but its velocity slows down to zero or even reverses, so the wavefront turns into the waveback. The dissipation of the front is caused by the inactivation of the Na current, and as such would look intuitively agreeable to physiologists and researchers working with detailed models. However, we should stress that the predominant view on the propagation failure is shaped by FHN-type thinking. An illustration of that can be found e.g. in the same paper mentioned above (Weiss et al. 2000), which states that “for a wave to break, its wavelength must become zero at a discrete point somewhere along the wave”. We will show here that although this picture is perfectly compatible with the behaviour of FHN-type systems, this is not what actually happens in realistic models.

Typically, if anything deviating from the FHN-type behaviour is observed in simulations of detailed models, this is usually understood as an inevitable consequence of the difference between simplified and detailed models. In this paper, we show that dissipation of excitation fronts *can* be understood and described in terms of simplified models, including analytical solutions.

The dissatisfaction with FHN-type systems for description of cardiac excitation has been felt for some time, and many alternative simplified models were suggested, either phenomenologically, or based on the structure of the detailed models, (Aliev & Panfilov 1996, Fenton & Karma 1998, Duckett & Barkley 2000, Bernus, Wilders, Zemlin, Verschelde & Panfilov 2002, Hinch 2002) to name a few. We did not find any of those simplified models sufficient for the purpose of this paper. However, the technique used by Hinch (2002) is rather close. For the convenience of the reader, we present our method in full, mentioning the difference in technique with Hinch (2002) in footnotes in relevant places in Section 3, and comparing the results in the Discussion.

The structure of the paper is as follows. Section 2 introduces the phenomenon of the wavefront dissipation by presenting results of numeric simulation of a selected detailed model of cardiac excitation, and explains why it is not possible in FHN-type systems. Section 3 presents in detail the construction of the new simplified model, which includes two steps, one asymptotic and one non-asymptotic. Section 4 presents exact wavefront solutions in the new simplified model and discusses their properties and implications. Section 5 presents results of numeric simulations of the new simplified model. Section 6 discusses the obtained results.

2 Preliminary observations

2.1 Initiation of an excitation wave and its failure

We start with a phenomenon well familiar to electrophysiologists, but not always so well to mathematical modellers dealing with simplified models: a local raise of the transmembrane voltage can initiate an excitation wave only if it is fast enough; a slow local increase does not trigger an excitation wave, even if the voltage rises to very high values. This is illustrated on fig. 1, where a model of the human atrial tissue suggested by Courtemanche, Ramirez & Nattel (1998) (CRN) was used, in which the equation for the voltage, analogous to the first equation of (1), was supplied with the following boundary conditions:

$$\frac{\partial E}{\partial x}(x_{\min}, t) = 0, \quad E(x_{\max}, t) = \min(E_{st} + kt, E_{\max}),$$

where E_{st} was the steady-state value of the voltage, E_{\max} was chosen close to the upper end of the physiological range, and the parameter k varied in different numeric experiments. As the results shown in fig. 1 suggest, the initiation of the excitation wave depends on the value of k , and the threshold value of k is between 0.19 and 0.20 mV/ms. The other pair of panels on fig. 1 demonstrates results of similar experiments with the FitzHugh-Nagumo system. Initiation of the excitation wave in the detailed model has a sharp threshold in terms of the rate of increase of the stimulating voltage. Whereas in the FHN system, it mainly depends on the absolute value of that voltage rather than its rate, and a 10-fold decrease of the rate only causes a 10-fold delay of the the wave initiation. This illustrates a qualitative difference between the real systems and their FHN caricature.

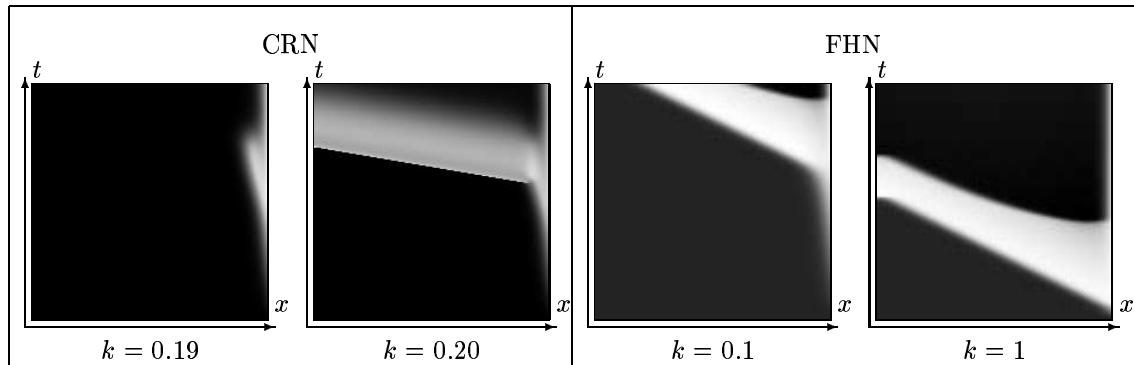


Figure 1: Initiation of an excitation wave in the biophysically detailed model (Courtemanche et al. 1998) (CRN) and FitzHugh-Nagumo model (1) (FHN), by raising the voltage on the right end of the cable with different speeds $k = (dE/dt)_{x_{\max}}$. Solutions are represented by shades of gray: black is the smallest value of E and white is the largest value of E within the solution. In CRN model: time range 10^3 ms, space range 250 s.u., $E_{st} = -81.18$ mV, $E_{\max} = 20$ mV; all the kinetic parameters are as in (Courtemanche et al. 1998). In FHN model: time range 50, space range 20, $\beta = 1.3125$, $\gamma = 0.5$, $\epsilon_E = 0.3$, $\epsilon_v = 0.03$, $E_{st} = -1.5$, $E_{\max} = 1.91$.

2.2 Two different mechanisms of propagation block.

This upstroke rate threshold for initiation of excitation waves in realistic models, being itself a well known fact, has a consequence that is less known and a lot less understood: a specific mechanism of termination of excitation wave, through a block of propagation. A typical scenario of propagation block in heart is that an excitation wave propagates where the tissue has not fully recovered after the previous wave, which may be because the wave is premature, or the tissue at that site has an abnormally long recovery period at that site. In that situation, a recovery wave moves before the

new excitation wave. If the recovery wave is slower than the excitation wave, the latter runs into more and more unfavourable condition and may eventually fail to propagate at all. This happens differently in realistic models and in FHN-type caricatures. This is illustrated on fig. 2 using an ultimate idealization of the excitability completely but temporarily suppressed in a part of the medium. This was done for the CRN model and the FHN system (1). In reality, the excitability is modulated by various slow variables such as the ionic concentrations, determining the reversal potentials of the ionic currents, and the slow gates, among which the most important is gate j which modulates the largest current, the fast Na current. However, simulation of the temporal block by j is complicated by the fact that its evolution is actually governed by a differential equation. Therefore, we have simulated the temporal excitability block in the CRN model by a change of the maximal conductivity of the Na channels, g_{Na} , which is a multiplier of j . In the FHN system, we have simulated the block of excitability by reducing to zero of the parameter ϵ_E which is the closest analogue of g_{Na} in that system of equations.

In the CRN model, when the conditions for propagation are restored, the excitation wave does not resume, as the sharp increase in the voltage necessary to trigger such wave is not present. Subsequent spread of the voltage is purely diffusive. In the FHN system, the high voltage at the front itself is enough to excite new cells if other conditions are right again; so the excitation front can propagate with arbitrarily slow speed or even stop, without dissipation. When propagation conditions are restored, the excitation wave resumes, even if the front near the edge of the inexcitable border has been smeared out by diffusion. The FHN wave will not resume only if the block lasts longer than the action potential, so the back of the wave reaches the block site and the whole excitation wave decays. On the contrary, the CRN wave loses the ability to propagate within milliseconds, long before the end of the action potential.

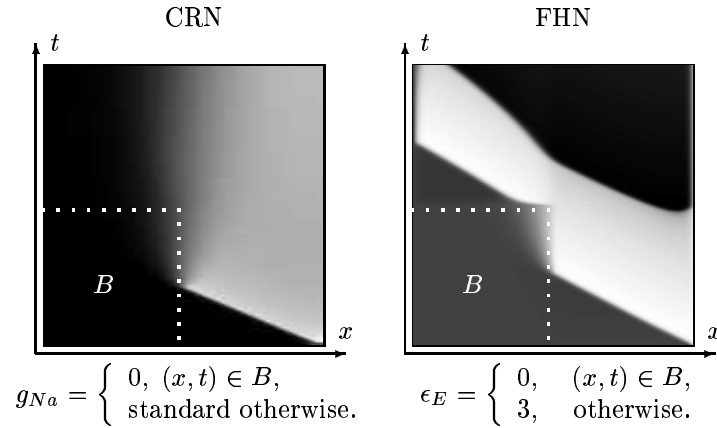


Figure 2: Temporary local block of the excitation front: the excitability of the medium is suppressed for $(x, t) \in B = (0, x_b) \times (0, t_b)$, where x_b and t_b are the middles of the space and time intervals (shown by the white dots). Here and below, solutions are represented by shades of gray: black is the smallest value of E and white is the largest value of E within the solution. In CRN model: time range 80 ms, space range 50 s.u. (space units, chosen so that $D = 1 \text{ su}^2\text{ms}^{-1}$), all the kinetic parameters are as in (Courtemanche et al. 1998). In FHN model: time range 50, space range 50, $\beta = 0.75$, $\gamma = 0.5$, $\epsilon_v = 0.03$.

2.3 Excitation fronts in FHN-type systems do not dissipate.

If $\epsilon_v \ll \epsilon_E$, system (1) belongs to a class of systems

$$\frac{\partial E}{\partial t} = \frac{\partial^2 E}{\partial x^2} + f(E, v), \quad (2)$$

$$\frac{\partial v}{\partial t} = \epsilon g(E, v), \quad 0 < \epsilon \ll 1, \quad (3)$$

($v \in \mathbb{R}^m$, $m \geq 1$), which we will call here FHN-type systems. For this class of systems, the asymptotic theory developed in 1970-1980s, see e.g. (Casten, Cohen & Lagerstrom 1975, Fife 1976, Rinzel & Terman 1982, Tyson & Keener 1988), can be applied. It is assumed that in a region of v , function $f(E, v)$ has three simple roots in E , $E_-(v)$ (recovery) $< E_*(v)$ (threshold) $< E_+(v)$ (excitation), where recovery and excitation are stable, $\frac{\partial f}{\partial E}(E_{\pm}(v), v) < 0$, and the threshold is unstable, $\frac{\partial f}{\partial E}(E_*(v), v) > 0$. Propagation of fronts and backs of excitation waves in the limit $\epsilon \rightarrow +0$ is described by trigger waves in the (2) with $v = \text{const}$. If the positive direction of propagation is to the left, the profile of a stationary trigger wave $E(x + ct)$ is a solution of the boundary-value problem

$$E'' + cE' + f(E, v) = 0; \quad E(\pm\infty) = E_{\pm}(v). \quad (4)$$

This is a trigger wave from the lower (recovery) stable equilibrium $E_-(v)$ to the higher (excitation) stable equilibrium $E_+(v)$ propagating with a speed which is a function of v , $c = c(v)$. The sign of $c(v)$ coincides with the sign of $\int_{E_-(v)}^{E_+(v)} f(E, v) dE$ and thus may change as v changes, i.e. a wavefront may stop and reverse to become a waveback. E.g., if $f(E, v) = a(v)(E - E_-(v))(E - E_*(v))(E_+(v) - E)$, then $c = (a/2)^{1/2} (E_+ + E_- - 2E_*)$ (Zel'dovich & Frank-Kamenetsky 1938, McKean 1970, Murray 1989).¹, or if $f(E, v) = -E + \theta(E - E_*(v))$, where $\theta()$ is the Heaviside step function, then $c = (1 - 2E_*)[E_*(1 - E_*)]^{-1/2}$ (McKean 1970). A solution to (4) represents the front of the excitation wave if $c(v) > 0$ and the back of the excitation wave if $c(v) < 0$. Between these trigger waves, E remains close to one of the two stable equilibria corresponding to the local value of the slow variables, $E(x, t) \approx E_{\pm}(v(x, t))$, and the evolution of these slow variables is therefore described by

$$v_t = \epsilon G_{\pm}(v), \quad G_{\pm}(v) \equiv g(E_{\pm}(v), v). \quad (5)$$

For a given evolution of the slow variables $v(x, t)$, the motion of the wavefront/waveback $X(t)$ on the large scale is described by an ordinary differential equation,

$$\frac{dX}{dt} = -c(v(X, t)) = -C(X, t). \quad (6)$$

By this equation, the front propagation speed $c(t) = c(v(X(t), t))$ changes according to

$$\frac{dc}{dt} = \frac{\partial C}{\partial t} - c \frac{\partial C}{\partial x}. \quad (7)$$

If we consider the front of the excitation wave, i.e. $c > 0$, then typically, whatever the history, the medium ahead of the front “restores the excitability”, i.e. $\partial C / \partial t > 0$. This means that for any spatial profile of $C(x, t)$ at the moment when $c = 0$, we have $dc/dt > 0$, thus c can not become negative. Note that if $v(x, t)$ evolves according to (5) (which is guaranteed if ϵ is very small) and is a one-component vector (as in the original FHN system), then the time-dependence of $v(x, t)$ at each x is monotonic in the intervals between fronts and backs. Thus, we have the following

Proposition 1 *In a FitzHugh-Nagumo-type system with a normal recovery process, the excitation wave front never stops completely. When approaching a region unfavorable for propagation, it slows down until the propagation conditions recover, and then proceeds further.*

If $\partial C / \partial t < 0$ does happen, which is possible if ϵ is not too small or the variable v is a vector rather than scalar, then c may become negative. In that case we will observe turning of the excitation wavefront into the waveback, moving in the opposite direction. This is also absolutely different from the dissipation of the front as shown in fig. 2 for the cardiac tissue model.

Proposition 2 *In a FitzHugh-Nagumo-type system with an abnormal recovery process, the worsening of propagation condition ahead of the front may cause it to stop, turn into wave back and move in the opposite direction.*

¹ McKean (1970) ascribed this solution to Huxley, but did not provide exact reference. Zel'dovich & Frank-Kamenetsky (1938) did not present the front solution itself, but gave the correct expression for the speed, which could only be obtained from the correct solution.

In any case, as long as v evolves so that the system remains excitable, i.e. $f(E, v)$ has its three roots in E , the sharp structure of the front given by (4) is preserved. This means that the front dissipation as seen in the realistic heart tissue models does not happen in FHN-type systems. A possible exception is that for $m = \dim(v) \geq 2$ the branch of $E = E_+(v)$ may be connected to the branch of $E = E_-(v)$ via an unexcitable, ‘monostable’ region of v where $f(E, v)$ has only one root in E . This is possible if the projection of the manifold $f(E, v) = 0$ to the $\{v\}$ space has a cusp singularity (Zeeman 1972). The analysis from this viewpoint of the Hodgkin & Huxley system has shown that although such singularity may be possible at some parameters, it is not likely to affect the behaviour of the system in realistic situations (Suckley & Biktashev 2003). So, although this possibility deserves a theoretical consideration, answers that are more practical can be obtained by considering real structure of realistic models. We do this in the rest of the paper, using one of the recent cardiac excitability models as an example.

3 Constructing the simplified model of the excitation front.

The difference in the behaviour of the realistic models and the FHN-type systems is not very surprising, since as we have mentioned neither the FHN system (1) nor any of its modifications (2,3) were obtained from the realistic models but were invented to simulate selected phenomenology. Thus, to derive a simplified model retaining the needed qualitative features, in our case, the front dissipation property, we start from a real system and make clearly defined simplifications with a view to retain this feature.

As an example of a realistic model we consider the CRN model (Courtemanche et al. 1998), the spatially one-dimensional form of which is

$$\begin{aligned}\frac{\partial E}{\partial t} &= D \frac{\partial^2 E}{\partial x^2} + g_{Na}(E_{Na} - E)m^3hj + \sum_k I_k, \\ \frac{\partial m}{\partial t} &= (\bar{m}(E) - m)/\tau_m(E), \\ \frac{\partial h}{\partial t} &= (\bar{h}(E) - h)/\tau_h(E), \\ \frac{\partial j}{\partial t} &= (\bar{j}(E) - \textcolor{yellow}{j})/\tau_j(E),\end{aligned}\tag{8}$$

where E is the transmembrane voltage, D is its diffusion coefficient, equal to intercellular conductivity per membrane capacitance, g_{Na} is the maximal specific conductivity per membrane capacitance of the fast Na current, E_{Na} is the reversal potential of that current, m , h and j are probability densities of the channel gates being open, \bar{m} , \bar{h} , \bar{j} are their instant equilibrium values, $\tau_{m,h,j}$ corresponding time scales, and $\sum_k I_k$ represents all other, smaller currents. Our purpose here is to derive a simplified model that would adequately describe the propagation not of the whole excitation wave, but only of its front. We need to develop a more realistic replacement of the fast (the first) equation in (1), leaving aside all other, slow dynamics corresponding to the dynamics of v in (1).

An immediate technical problem is that any asymptotic procedure, strictly speaking, applies not to a given system of equations, but to a family of systems depending on at least one parameter, to allow the limit when this parameter tends to zero or to infinity. However, the CRN model (8) does not depend on any parameters, but only contains constants, which have been measured experimentally and have certain values, even if not always known with a good precision. Of course, we might consider physiologically feasible variations of the experiment and/or of the tissue conditions, so that some of the constants of (8) become parameters that can vary from one experiment to another. However, this would only provide parameters varying in certain finite ranges, and none of them can be reasonably assumed tending to zero or to infinity. Thus, to apply the singular perturbation technique to our problem we need to introduce the small parameters

artificially. This is of course a standard practice in principle, but the particular way we do it here is not quite usual, so we are going to formalise this procedure, to avoid confusion.

Definition We will call a dynamical system

$$\dot{x} = F(x; \epsilon), \quad x \in \mathcal{X},$$

in a phase space \mathcal{X} , depending on a parameter ϵ , a *1-parametric embedding* of a dynamical system in the same space but without parameters,

$$\dot{x} = f(x), \quad x \in \mathcal{X},$$

if $f(x) \equiv F(x, 1)$ for all $x \in \mathcal{X}$. We define a *k-parametric embedding* by induction as a 1-parametric embedding of a system which itself is a $(k-1)$ -parametric embedding of the original system without parameters. If the parameter(s) ϵ are considered in a limit, say $\epsilon \rightarrow 0$, we call it an *asymptotic embedding*.

The typical use of asymptotic embedding has the form of a replacement of a small constant with a small parameter. If a system contains a dimensionless constant a which is “much smaller than 1”, then replacement of a with ϵa constitutes a 1-parametric embedding, and then the limit $\epsilon \rightarrow 0$ can be considered. In practice, constant a would more often be replaced with parameter ϵ , but technically speaking the limits $\epsilon \rightarrow 0$ and $\epsilon a \rightarrow 0$ are of course equivalent. A given system can have infinitely many asymptotic embeddings, and which of them is better depends on the qualitative features of the original system that need to be represented, or classes of solutions that need to be approximated by the asymptotics. In this paper, we suggest a parametric embedding of the realistic models of cardiac excitation, using the CRN model as an example, with the aim to reproduce the solutions for the *fronts*, without paying attention to any other features (say, shape of the action potential etc). In realistic models, the front of an excitation wave is characterised by a rapid growth of E , due to the large magnitude of the Na current. Bearing this in mind, we identify the following features in the model, which will provide us with the possibility of introducing artificial small parameters:

- The maximal value of all the small currents $\sum_k I_k$ put together is much smaller than the typical value of the Na current for the solutions of interest. That gives one small parameter, ϵ_1 .
- Functions $\bar{m}(E)$ and $\bar{h}(E)$ are nearly stepwise functions. In particular, $\bar{m}(E)$ is small (not exceeding a small constant δ) for E below a certain E_m^δ , and $\bar{h}(E)$ is small (not exceeding a δ) for E above a certain E_h^δ . This makes two more small parameters, ϵ_2 and ϵ_3 .
- The typical values of $\tau_m(E)$ are much smaller, and $\tau_j(E)$ are much larger than $\tau_h(E)$ and g_{Na}^{-1} . This makes two more small parameters, ϵ_4 and ϵ_5 .

The corresponding parametric embedding can be taken in the form

$$\begin{aligned} \frac{\partial E}{\partial t} &= D \frac{\partial^2 E}{\partial x^2} + g_{Na}(E_{Na} - E)m^3 h j + \epsilon_1 \sum_k I_k, \\ \frac{\partial m}{\partial t} &= [(1 - \epsilon_2 \delta)m_0^\delta(E) + \epsilon_2 \delta m_1^\delta(E) - m] / (\epsilon_4 \tau_m(E)), \\ \frac{\partial h}{\partial t} &= [(1 - \epsilon_3 \delta)h_0^\delta(E) + \epsilon_3 \delta h_1^\delta(E) - h] / \tau_h(E), \\ \frac{\partial j}{\partial t} &= \epsilon_5 [\bar{j}(E) - j] / \tau_j(E), \end{aligned} \tag{9}$$

where

$$m_1^\delta(E) = \delta^{-1} \min(\delta, \bar{m}(E)), \quad m_0^\delta(E) = (1 - \delta)^{-1} \theta(E - E_m^\delta) (\bar{m}(E) - \delta), \quad \bar{m}(E_m^\delta) = \delta,$$

so that

$$\inf(m_{0,1}^\delta(E)) = 0, \quad \sup(m_{0,1}^\delta(E)) = 1, \quad (1 - \delta)m_0^\delta(E) + \delta m_1^\delta(E) = \bar{m}(E), \quad m_0(E > E_m^\delta) = 0,$$

and, similarly,

$$h_1^\delta(E) = \delta^{-1} \min(\delta, \bar{h}(E)), \quad h_0^\delta(E) = (1 - \delta)^{-1} \theta(E_h^\delta - E)(\bar{h}(E) - \delta), \quad \bar{h}(E_h^\delta) = \delta,$$

and

$$\inf(h_{0,1}^\delta(E)) = 0, \quad \sup(h_{0,1}^\delta(E)) = 1, \quad (1 - \delta)h_0^\delta(E) + \delta h_1^\delta(E) = \bar{h}(E), \quad h_0(E < E_h^\delta) = 0.$$

Of all the five limits $\epsilon_l \rightarrow 0$, only $\epsilon_4 \rightarrow 0$ is singular. In the leading term, it means that m gate is a fast variable and should be adiabatically excluded by replacing it with its quasistationary value, $m = \bar{m}(E)$. The other four limits are regular, in the sense that the leading order can be obtained by simply replacing ϵ_l by zeros.² This, in particular, changes the quasistationary value of $m = \bar{m}(E)$ to

$$m = m_0^\delta(E). \quad (10)$$

At $\epsilon_5 = 0$, the right-hand side of the equation for j vanishes, and we have

$$j = \text{const} \quad (11)$$

throughout the front. The remaining two equations become

$$\frac{\partial E}{\partial t} = D \frac{\partial^2 E}{\partial x^2} + I_{Na} (m_0^\delta(E))^3 h, \quad (12)$$

$$\frac{\partial h}{\partial t} = (h_0^\delta(E) - h)/\tau_h(E), \quad (13)$$

where $I_{Na} = g_{Na}j(E_{Na} - E)$. System of two equations (12,13) is the fast subsystem corresponding to the full system (8), and describing the front of the wave, leaving the slow processes, such as action potential plateau and recovery, out of the scope.³ In this capacity, it is similar to (2), one fast equation with respect to the whole system. But there is another significant difference, apart from two equations vs one. The limits $\epsilon_2 \rightarrow 0$ and $\epsilon_3 \rightarrow 0$, despite being formally regular, make a dramatic change to the properties of the system, because of the special character of the functions $m_0^\delta(E)$ and $h_0^\delta(E)$. Namely, the spatially homogenous steady states in (12,13) are not isolated, as in (2), but form two continua: $\{(E, h) | E \in (-\infty, E_h^\delta] \cup [E_m^\delta, +\infty), h = h_0^\delta(E)\}$. These two continua correspond to complete closure of either m or h gates. This complete closure is possible due to m_0^δ and h_0^δ being exactly zero in the corresponding intervals of E .

The equilibria with $E \in (-\infty, E_h]$ correspond to the possible state of the medium before the front, when all m gates are still closed, and equilibria with $E \in [E_m, +\infty)$ to possible state after the front, where all h gates are already closed. Thus, we are interested in front solutions where one asymptotic state belongs to one continuum, and the opposite asymptotic state belongs to the other. This poses a problem of selection of the states. It is natural to assume that the pre-front voltage is determined by the state of the medium through which the front propagates.⁴ Which, if any, post-front voltages may correspond to a given pre-front voltage, and what may be corresponding front speed(s), are questions that can be answered by studying appropriate solutions of (12,13).

² Hinch (2002), although considering $\sum I_k$ small, retained it in the simplified model, i.e. did not put ϵ_1 to zero. The small currents, which in the detailed model are described by a system of 17 differential equations, he represented phenomenologically, in terms of linear active resistance with respect to the resting potential.

³ Hinch (2002) has retained the process of slow recovery in the simplified model, through the phenomenologic small current with the reversal potential of the resting potential.

⁴ In (Hinch 2002), the pre-front voltage is always the resting potential, i.e. a single point instead of the continuum $(-\infty, E_h^\delta)$, despite the fact that the gates are assumed perfect switches, too. This is because of the retained small currents of the resting potential. Thus, propagation through a not completely recovered tissue or in models where there is no resting potential (e.g. Purkinje fibres) are out of the scope of that model.

This, normally, would be done numerically. But before attempting that, it would be helpful to know at least some qualitative answers, e.g. how many different front solutions might exist at a given pre-front voltage. The classical theory of excitable media, developed for FHN-type systems is useless in this case, but provides encouraging examples in the form of exact front solutions for special ‘caricature’ form of nonlinearities, cubic (Zel’dovich & Frank-Kamenetsky 1938) and piecewise linear (McKean 1970). Cubic, or any analytical form of nonlinearities for (12,13) is clearly impossible, so in this paper, we build a piece-wise linear variant of this system, and find the exact front solution.

Thus, from now on expecting only qualitative but not necessarily quantitative agreement with reality, we do further two simplifications:

- We note that $m_0^\delta(E)$ and $h_0^\delta(E)$ are step-like functions, taking values strictly equal to 0 in one limit and fastly approaching 1 in the opposite limit. We replace them with

$$m_0^\delta(E) = \theta(E - E_m) = (m_0^\delta(E))^3 \quad h_0^\delta(E) = \theta(E_h - E),$$

where $\theta()$ is the Heaviside step function. This “approximation” can be done to the original functions $\bar{m}(E)$ and $\bar{h}(E)$, say by choosing E_m and E_h so that $(\bar{m}(E_m))^3 = \bar{h}(E_h) = 0.5$ (see fig. 3). For CRN model, this gives $E_m \approx -33$ mV and $E_h \approx -67$ mV.⁵

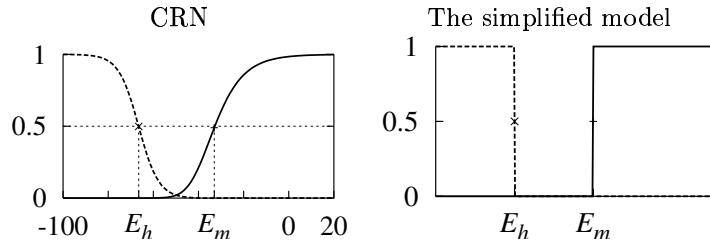


Figure 3: Dependence of $\bar{m}^3(V)$ and $\bar{h}(V)$ for the Courtemanche et al. (CRN) (Courtemanche et al. 1998) detailed model and for the proposed simplified model (14).

- Further, we replace functions $\tau_h(E)$ and $I_{Na}(E)$ by constants as their dependence on E is not essential for the purpose of the present qualitative analysis. This step may be least obvious for $I_{Na}(E)$. One objection that many would put forward is that $I_{Na}(E)$ has a root at $E = E_{Na}$, which, in particular, means that the transmembrane voltage never exceeds E_{Na} ; so replacing this function with a constant changes the properties of the system qualitatively. Our justification for such replacement is based on the observation that in reality, the transmembrane voltage E hardly ever reaches values really close to E_{Na} , because growth of E stops when gates m or h close down, which happens long before I_{Na} vanishes. Thus, the maximum of the transmembrane voltage at the front is usually significantly lower than E_{Na} . For example, maximal E for fronts in the CRN model propagating through a completely recovered medium is $E_{\max} \approx +5$ mV which is by more than 60mV lower than $E_{Na} \approx +67$ mV. This, by the way, is a compelling reason to consider the dynamics of h as equally fast to those of E : if say E was considered as a faster variable, then the post-front voltage would be fixed to E_{Na} , i.e. much higher than it is in reality. Dependence of I_{Na} on E is through the factor $E_{Na} - E$. And the relevant range of voltages is from E_m , the minimal voltage at which Na current becomes possible, to E_{\max} , above which the voltage never rises. Within this range, the factor $E_{Na} - E$ changes only by about 1.6 times.⁶ In contrast, function

⁵ Hinch (2002) has taken the threshold voltages E_m and E_h equal to each other. We believe that while slightly simplifying the solution, this assumption is not very realistic and leads to a significant difference in the results, see below.

⁶ Hinch (2002) did not replace function I_{Na} with a constant but kept in the form $I_{Na} = g_{Na}j(E_{Na} - E)$. The front solutions still can be found analytically, but require modified Bessel functions. Considering that variation $\tau_h E$ is much larger than $I_{Na}(E)$, this complication does not seem to be worthwhile.

$\tau_h(E)$ within the relevant region from E_h to E_{\max} changes between 28 ms and 0.16 ms, so replacement of this function with a constant is more likely to cause numerical discrepancy with the accurate model.⁷

Having done these simplifications, we obtain the following piecewise-linear system of equations,

$$\begin{aligned}\frac{\partial E}{\partial t} &= D \frac{\partial^2 E}{\partial x^2} + I_{Na} \theta(E - E_m) h, \\ \frac{\partial h}{\partial t} &= \frac{1}{\tau_h} (\theta(E_h - E) - h),\end{aligned}\tag{14}$$

which after change of variables $E = E_h + (E_m - E_h)\tilde{E}$, $t = I_{Na}^{-1}\tilde{t}$, $x = D^{1/2}I_{Na}^{-1/2}\tilde{x}$, $\tau = I_{Na}\tau_h$, and omitting the tildes, becomes finally

$$\begin{aligned}\frac{\partial E}{\partial t} &= \frac{\partial^2 E}{\partial x^2} + \theta(E - 1)h, \\ \frac{\partial h}{\partial t} &= \frac{1}{\tau} (\theta(-E) - h),\end{aligned}\tag{15}$$

depending on one dimensionless parameter, τ . The two continua of steady states in this model are $(E, h) \in (-\infty, 0] \times \{1\} \cup [0, +\infty) \times \{0\}$, which provide a variety of possible pre-front voltages $-\alpha$, a variety of post-front voltages ω , and a variety of corresponding speeds c .

4 The analytical results

4.1 The travelling front solutions

We will now analyse the newly proposed model (15). First of all, we consider solutions in the form of fronts propagating with constant speed and shape. A front propagating leftwards with speed c is represented by a solution depending only on the combination $\xi = x + ct$ and satisfying the automodel (“wave”) system of ordinary differential equations,

$$cE' = E'' + \theta(E - 1)h, \quad ch' = \frac{1}{\tau} (\theta(-E) - h).\tag{16}$$

This is supplied by auxiliary conditions:

$$\begin{aligned}E(-\infty) &= -\alpha < 0; & E(+\infty) &= \omega > 1; \\ h(-\infty) &= 1; & h(+\infty) &= 0.\end{aligned}$$

We choose the phase of the front so that $E(0) = 0$, denote $\xi_1 > 0$ the point where $E(\xi_1) = 1$, and require that $E(\xi)$ has a continuous derivative and $h(\xi)$ is continuous. This is in agreement with the fact that the right-hand sides of (16) are discontinuous, and implies corresponding internal boundary conditions at $\xi = 0$ and $\xi = \xi_1$. As (16) is piecewise linear, the solutions are found analytically. With the set auxiliary conditions, the problem has a family of solutions, in which one of the parameters (α, ω, c) can be chosen arbitrarily. A natural choice is α , as the voltage ahead of the front must be considered as given, when studying the front propagation. The family of solutions is

$$\begin{aligned}E(\xi) &= \begin{cases} -\alpha + \alpha \exp(c\xi) & (\xi \leq \xi_1), \\ \omega - \frac{\tau^2 c^2}{1 + \tau c^2} \exp\left(-\frac{\xi}{\tau c}\right) & (\xi \geq \xi_1), \end{cases} \\ h(\xi) &= \begin{cases} 1 & (\xi \leq 0), \\ \exp\left(-\frac{\xi}{\tau c}\right) & (\xi \geq 0), \end{cases}\end{aligned}\tag{17}$$

⁷ In (Hinch 2002), τ_h has different values below the threshold $E_m = E_h$ and above it. Still, the range of values of $\tau_h(E)$ in CRN is very large, even if only in the interval from E_m to E_{\max} .

where $\omega = 1 + \tau c^2(\alpha + 1)$, $\xi_1 = c^{-1} \ln(1 + \alpha^{-1})$ and speed c is an implicit function of τ and α , defined by

$$\tau c^2 \ln \left(\frac{(1 + \alpha)(1 + \tau c^2)}{\tau} \right) + \ln \left(\frac{\alpha + 1}{\alpha} \right) = 0, \quad (18)$$

which we will call the speed equation.

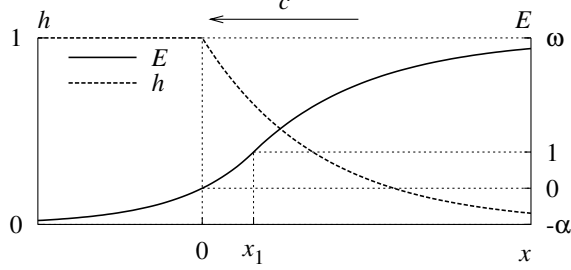


Figure 4: A propagating front solution (17,18) to (16) ($\tau = 8$, $\alpha = 1$, $c \approx 0.444$).

Note that here the post-front voltage ω depends on τ , a parameter in the equation for h ; this is another difference from the FHN-type systems where it only depends on the right-hand sides of the equation for E .

So, the front selection problem has the following solution: for every pre-front voltage $-\alpha$, the speed equation defines a discrete set of post-front voltages and corresponding speeds. How big is this discrete set we find out in the next section.

4.2 Properties of the speed equation.

Equation (18) can be rewritten in the form of an equation of level curves

$$\ln \tau = g(\beta, \sigma) \quad (19)$$

of the function

$$g(\beta, \sigma) \equiv \ln(1 + \sigma) - \ln(1 - \beta) - \sigma^{-1} \ln \beta,$$

where $\sigma = \tau c^2$, $\beta = \alpha/(\alpha + 1)$, $(\beta, \sigma) \in S = (0, 1) \times (0, +\infty)$.

It can be seen that

- For every fixed β , $\partial g / \partial \sigma$ changes sign once as σ runs through $(0, +\infty)$.
- Function $g(\beta, \sigma)$ has a local minimum $\sigma_* \approx 1.53659 \dots$, $\beta_* \approx 0.39423 \dots$, $g_* \approx 2.0378 \dots$, where $\sigma_*^2 = (\sigma_* + 1) \ln(\sigma_* + 1)$, $\beta_* = (\sigma_* + 1)^{-1}$ and $g_* = g(\beta_*, \sigma_*)$. This minimum has a non-degenerate quadratic form, and is the only critical point of g in S .
- Function $g(\beta, \sigma)$ has the following lower bounds

$$\begin{aligned} g(\beta, \sigma) &> \ln[\ln(1/\beta)], \quad g(\beta, \sigma) > \ln(1/(1 - \beta)), \\ g(\beta, \sigma) &> \ln(1/\sigma), \quad g(\beta, \sigma) > \ln \sigma, \quad \forall (\beta, \sigma) \in S. \end{aligned}$$

These observations are sufficient to describe qualitatively the behaviour of solutions of (19) for all τ . In the vicinity of the generic minimum (β_*, σ_*) the isolines of g are simple closed (approximately elliptic) curves. From the lower bounds, it can be seen that for any $C > g_*$, the isoline $g^{-1}(C) = \{(\beta, \sigma) | g(\beta, \sigma) = C\}$ is bounded within the rectangle $(\beta, \sigma) \in (\exp(-e^g), 1 - e^{-g}) \times (e^{-g}, e^g) \subset S$. By Theorem 3.1 from (Milnor 1963), as (β_*, σ_*) is the only critical point in S , isolines for all $C > g_*$ are homotopically equivalent to the isolines in the vicinity of (β_*, σ_*) , i.e. are simple closed curves surrounding (β_*, σ_*) . Furthermore, by the same theorem, if $C_1 < C_2$ then isoline $g^{-1}(C_1)$ lies within isoline $g^{-1}(C_2)$. Therefore, if there existed a point in S with $g < g_*$,

it would have to lie inside every isoline $g^{-1}(C)$, $C > g_*$, i.e. coincide with (β_*, σ_*) , which is impossible. Thus, (β_*, σ_*) is a global minimum in S . Since $\partial g / \partial \sigma$ changes sign only once, equation $g(\beta, \sigma) = C$ can have at most two solutions σ for every fixed β . Thus we have the following

Lemma 1 *Solutions of (19) are: (i) none for $\tau < \tau_* = e^{g_*} \approx 7.6740 \dots$, (ii) one point (β_*, σ_*) for $\tau = \tau_*$, (iii) a single closed curve surrounding (β_*, σ_*) and crossing each line $\beta = \text{const}$ at most twice, for every $\tau > \tau_*$.*

A selection of level curves is presented on fig. 5.

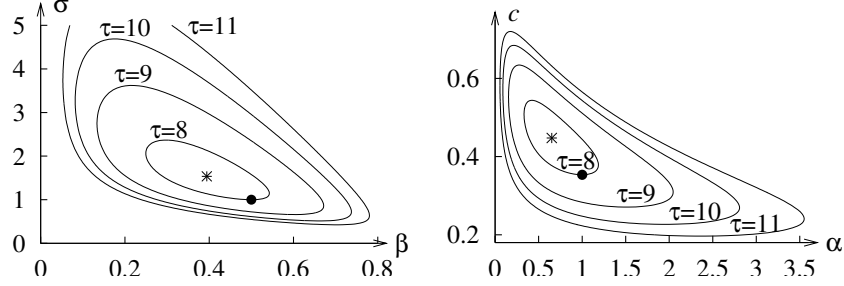


Figure 5: Pre-front voltage vs front speed for a selection of values of τ (labels on the curves), in (β, σ) coordinates, and in the original (α, c) coordinates. \bullet : exact solution $\beta = 0.5$, $\sigma = 1$, $\tau = 8$. $*$: the minimum of τ : $\beta_* \approx 0.394$, $\sigma_* \approx 1.537$, $\tau_* \approx 7.67$.

Thus, for every $\tau > \tau_*$, there exists a range of pre-front voltages $0 < \alpha_{\min}(\tau) < \alpha < \alpha_{\max}(\tau) < +\infty$, for each of which there are two propagating front solutions (17) with different speeds, and all propagation speeds possible at various pre-front voltages, span an interval $0 < c_{\min}(\tau) \leq c \leq c_{\max}(\tau) < +\infty$.

Explicit estimates can be obtained in the limit of large τ , e.g.

$$\alpha_{\min} = e^{1-\tau/e} \left(1 + \frac{5e}{2} \tau^{-1} + O(\tau^{-2}) \right), \quad c(\alpha_{\min}) = e^{-1/2} \left(1 - \frac{e^2}{4} \tau^{-2} + O(\tau^{-3}) \right), \quad (20)$$

$$\alpha_{\max} = \tau \left(1 - 2 \tau^{-1/2} + O(\tau^{-1}) \right), \quad c(\alpha_{\max}) = \tau^{-3/4} \left(1 + \frac{3}{4} \tau^{-1/2} + O(\tau^{-1}) \right), \quad (21)$$

$$\alpha(c_{\min}) = e^{-1} \tau \left(1 - \frac{3e}{2} \tau^{-1} + O(\tau^{-2}) \right), \quad c_{\min} = e^{1/2} \tau^{-1} \left(1 + \frac{3e}{4} \tau^{-1} + O(\tau^{-2}) \right), \quad (22)$$

$$\alpha(c_{\max}) = \tau^{-1} \left(1 + \frac{\ln \tau + 2}{\tau} + O(\tau^{-2} \ln^2 \tau) \right), \quad c_{\max} = 1 - \frac{\ln \tau + 2}{2\tau} + O(\tau^{-2} \ln^2 \tau), \quad (23)$$

$$c(\alpha) \approx (\alpha + 1)^{-1/2} (1 + O(\tau^{-1})) \quad (\alpha = O(1)). \quad (24)$$

The boundedness of possible propagation speeds from below has a special significance. If the excitation front propagates through medium that is in the process of recovery, it can not propagate faster than medium ahead of it recovers. And if the speed of medium recovery is slower than c_{\min} this means that propagation of the front becomes impossible (actually the minimal speed is even higher than that, see below), and in this case the front dissipation becomes inevitable.

5 Numerical results

5.1 Fast and slow waves

For every admissible pair of τ and α , with the exception of the marginal values of α , equation (18) gives two different values of the speed c . This means possibility of propagation of two different kinds of excitation fronts through the same pre-front state of the medium, differing from each

other by their speed and post-front voltages. This is very different from FHN-type systems, where the front solution in (2) is unique for every set of values of the slow variables.

So, there is a question, which of the two front solutions will realise in a particular propagating wave. Numerical experiment suggests that it is always the faster solution, with the higher post-front voltage. Fig. 6 shows results of numerical simulations of the simplified model (15) with initial conditions specified by (17) where speed c was taken as either of the two solutions of the speed equation (18). Simulations shown in panels (a) and (b) correspond to two approximations the slower solution, and simulation of panel (c) corresponds to the faster solution. The values of c in (a) and (b) differ from each other in the fourth significant figure. Both simulations (a) and (b) show propagation of the excitation front described by (17) for some time, but eventually it is destroyed. On panel (a), the front has dissipated. On panel (b), it has developed into a stronger and faster front. This stronger and faster front corresponds to the faster solution of (18) and is identical, up to the initial phase, to the solution shown on panel (c).

Numerical simulations with selected other values of τ and α showed similar results. Thus, the numerical experiment suggests that the slow front solutions are always unstable. This can be verified by the linear stability analysis; we leave this question for future study. If this conjecture is true, then in every level curve of function $g(\beta, \sigma)$ in fig. 5, only its upper half corresponds to stable fronts. The locus of marginal points in the (β, σ) plane, where the fast and slow solutions join, is given by condition $\partial g(\beta, \sigma)/\partial \sigma = 0$. In terms of the original variables α, c , this gives the following stability condition,

$$\tau^2 c^4 + (1 + \tau c^2) \ln(1 + \alpha^{-1}) > 0, \quad (25)$$

in addition to the speed equation (18). The minimal propagation speed at a given value of τ is then given not by $c_{\min} = O(\tau^{-1})$ which is unattainable as the corresponding front is unstable, but by $c(\alpha_{\max}) = O(\tau^{-3/4})$.

Note that existence of two solutions with different speeds, with the slower solution unstable and faster solution stable, is a well-known property of pulses in FHN-type systems. The difference is that in the new simplified model, the two solutions have not only different speeds and shapes, but, unlike pulses in FHN-type systems, have different $t \rightarrow +\infty$ asymptotic states.

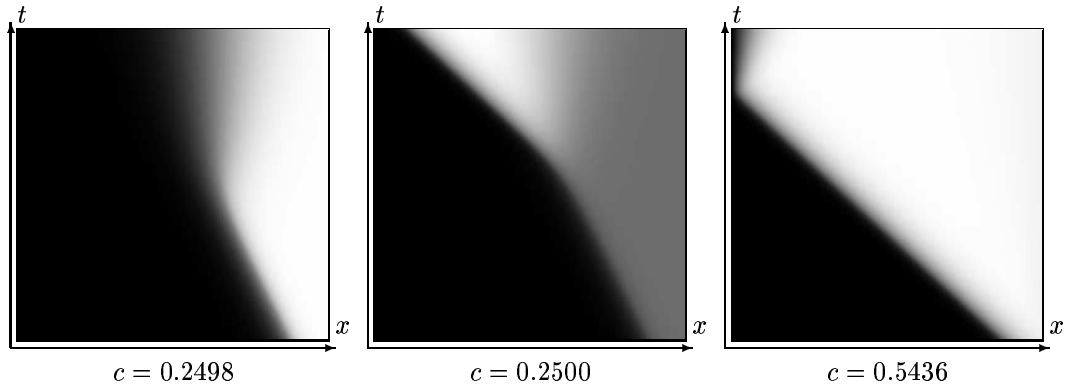


Figure 6: Solutions of (15) with initial conditions (17), for $\tau = 10$, $\alpha = 1$ and c close to the two solutions of (18). Space range is 100, time range is 200. Depending on minute details, the slow front either dissipates or develops into the faster front, corresponding to $c \approx 0.5436$.

5.2 Temporary block of excitability

To verify that the new simplified model reproduces the phenomenon of wavefront dissipation for which it was designed, we have performed simulations of (15) in conditions similar to those shown in fig. 2, i.e. temporarily suppressed excitability in a part of the medium. The analogue of

parameters g_{Na} and ϵ_E in the simplified model is τ . According to the analytical results obtained, the excitability is observed for $\tau > \tau_* \approx 7.674\dots$. To make the effect more prominent, we choose the excitable part of the medium with τ slightly above the threshold, $\tau = 8$, and the suppressed excitability slightly below the threshold, $\tau = 7$. The results are shown on fig. 7. The front dissipated soon after it reached the blocked region; the short period of decaying propagation is due to the fact that the excitability is only slightly below the threshold. After that, the front disappears and further spread of the voltage is purely diffusive. When excitability in that region was restored, the front did not resume but continued to spread diffusively. So, the new model describes the wavefront dissipation, similarly to the detailed equations and different from the FHN model. The prediction of the analytical theory about the excitability threshold τ_* is confirmed by direct numerical simulation.

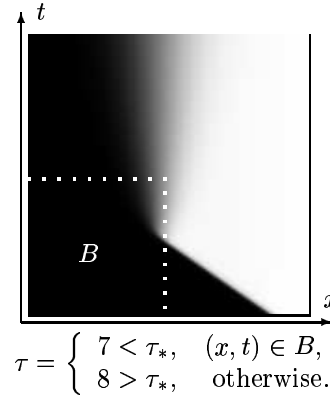


Figure 7: Temporary local block (B , white dots) of the excitation front in the simplified model (15), as in fig. 2. Front propagation did not resume after the excitability has been restored. Initial conditions (17) with $\tau = 8$, $\alpha = 1$, $c = 0.444$. Time range 1000, space range 300.

6 Discussion

Excitation fronts in realistic models of biological excitable media can not be stopped or reversed. If they are not allowed to propagate, they dissipate. This makes them different from the FHN-type caricatures, where fronts can slow down indefinitely or reverse and turn into the wavebacks. Local propagation blocks can break excitation waves and are essential in fibrillation. An established belief, based on FHN-type models and expressed e.g. by Weiss et al. (2000), is that a wavebreak happens when the waveback catches up with the wavefront and the length of the excitation wave becomes zero. As we now see, in realistic models the wavelength is irrelevant and whether or not the wave breaks is decided exclusively (in the asymptotical sense) by events in its front.

The key process responsible for dissipation of the front is the closure of the slow Na gate h . Thus any asymptotic approach intended to describe adequately front propagation at slow speed or its failure, must take the dynamics of h into account, alongside with the dynamics of the transmembrane voltage E . Our simplified model shows that this is necessary even if the ratio of characteristic time scales of E and h is rather high, say around 8.

The proposed simplified model (15) captures the main features of realistic models responsible for the propagation and dissipation of the excitation fronts. This model provides exact analytic solution for the front shape (17) and speed (18). This solution provides description of a number of qualitative features:

1. Front parameters, including propagation speed, are determined by the pre-front value of the transmembrane voltage E through the dimensionless parameter α , and by the local value of the sodium reversal potential E_{Na} and slow sodium inactivation gate j , through the dimensionless excitability parameter τ .

2. The range of pre-front voltages $-\alpha$, at which propagation is possible at a given τ , is bounded from below and from above.
3. The range of values of excitability parameter τ , at which propagation is possible at a given α , is bounded from below.
4. There is a minimal value τ_* of the excitability parameter τ , at which propagation is possible at any α at all.
5. For every admissible pair of α and τ except the marginal values, there exist two front solutions with different speeds. Numerical experiment suggests that the faster front solution is stable and the slower front solution is unstable.
6. At a given τ , dependence of the faster (stable) front speed on the pre-front voltage $-\alpha$ is non-monotonic: it is maximal at an intermediate value of α and decreases as α approaches its limits.
7. The range of possible propagations speeds, as well as the range of speeds of stable fronts, at a given τ and variable α are bounded from below and from above.
8. The range of possible propagations speeds at a given α and variable τ is bounded from below and from above in dimensionless units. In the original dimensional units, however, there is no upper limit of speed and it grows as $\tau^{1/2}$ at large τ .

Some of these features are well known, other can be easily compared with numerical simulations of the detailed models. Direct comparison with experiments is, as always, more difficult. Feature 6, i.e. non-monotonic dependence of propagating speed on the pre-front voltage, agrees with experimental observations of propagation speed dependence on the resting potential in guinea pig ventricle (Kagiyama, Hill & Gettes 1982). Recent experimental observation by Aliev, Baudenbacher, Baudenbacher & Wikswo (2002) of slow and low-amplitude excitation waves that are initiated by special stimulation protocol and then either dissipate or develop into fast large-amplitude waves, although admitting different explanations, are consistent with feature 5 and numerical simulations shown on fig. 6. As Hinch (2002) comments, feature 8 does not agree with the experimental dependence of maximal speed less steep than $O(\tau^{1/2})$, which is probably an artifact of the singular limit $\epsilon_4 \rightarrow 0$.

As we discussed in Section 3, there are infinitely many embeddings, i.e. ways in which artificial small parameters may be introduced, for a given detailed model. It is therefore interesting to compare the features of solutions obtained in different embeddings of the same class of models. Hinch (2002), addressing the problem of propagation block, mainly in the context of critical curvature for modelling the WPW syndrome, has considered a series of semi-phenomenological simplified models one of which in many aspects is similar to the one considered here. One significant difference was that Hinch restricted consideration only to fronts propagating through a fully recovered medium, so the pre-front voltage always corresponded to the resting state, and thus is a parameter of the model not of the solution. Therefore, feature 1 looks different in his model and features 2, 4, 6, 7 simply cannot be compared as they are beyond the scope of Hinch's approach. Another significant difference in the results is that the minimal propagation speed in the Hinch's simplified model depends on the small sub-threshold currents (i.e. all currents but the fast sodium current), in such a way that in the limit that these currents vanish, i.e. the very limit we consider here, this minimal propagation speed vanishes, too. More accurately, the minimal speed is $\propto g_c^{1/4}$ as the conductivity of the subthreshold current $g_c \rightarrow +0$, i.e. can be noticeable even for rather small g_c . Still, formally the difference with our model is essential, and it would be interesting to investigate which of the differences in the two approaches has caused this difference in the results. Our guess is that it is Hinch's assumption that $E_m = E_h$. If that is so, it poses a question of what may be the evolutionary advantages of the inequality of $E_m > E_h$, as one disadvantage is already apparent: this inequality is a pre-requisite of the existence of the macroscopic minimal speed of

the excitation front, and is therefore responsible for the excitation wave being less robust than it would be at $E_m = E_h$.

The main qualitative results of the analysis of the simplified model are the conditions of existence of propagating front solutions, as their violation implies propagation block and front dissipation. This violation may be caused by interaction of the spatio-temporal variation of the distribution of relevant tissue parameters contributing to model parameters α and τ , and the front movement through medium with these distribution. A simple sufficient criterion of front dissipation can be given in terms of the front propagation speed. In the scenario described in Section 2.2, if the recovery wave before the excitation front moves slower than the slowest speed with which the front may move, the front will dissipate. The estimate of the critical speed may be c_{\min} or, if the conjecture about front stability is correct, $c(\alpha_{\max})$. The condition on speed is a sufficient, but not a necessary condition of the front dissipation. Other causes of dissipation may be if the existence conditions of front solution are violated in any other way, or if the front solution exists but the initial/boundary condition are not appropriate to initiate it, as results of numerical simulations on figs. 6 and 7 show.

The model (15) or its dimensional version (14) can not produce quantitatively accurate results, particularly because of the simplifications made in transition from (12,13) to (14). The crudest of those is the replacement of $\tau_h(E)$ with a constant despite its variation in the relevant range of E by about two orders of magnitude. Yet, it may be interesting to consider at least some estimates. Taking for the CRN model $E_h = -67$ mV, $E_m = -33$ mV, $E_{Na} = +67$ mV, and estimating $I_{Na}(E)$ and $\tau_h(E)$ by their value at $E_{\max} = +5$ mV, we get $I_{Na} \approx 630$ ms⁻¹, $\tau_h \approx 0.16$ ms, and, assuming $j = 1$, the excitability parameter $\tau = I_{Na}\tau_h \approx 100$. Thus in normal fully recovered tissue, the excitability parameter exceeds the propagation threshold by an impressive safety factor of $\tau/\tau_* \approx 13$. The pre-front parameter, corresponding to the resting state $E_{st} \approx -81$ mV is $\alpha = (E_m - E_{st})/(E_m - E_h) \approx 1.44$, so the estimate of the dimensionless speed is then $\tilde{c} \approx (\alpha + 1)^{-1/2} \approx 0.64$. The dimensional speed is $c = \tilde{c}(DI_{Na})^{1/2}$ which for $D = 3 \cdot 10^{-5}$ mm²/ms gives $c \approx 0.13$ mm/ms against 0.26 mm/ms provided by direct numerical simulation of the full CRN model with this D . The absolute minimal propagation speed is $\tilde{c}_{\min} \approx e^{1/2}\tau^{-1} \approx 0.016$, i.e. roughly 10 times slower than the normal speed, and the minimal stable propagation speed is $\tilde{c}(\alpha_{\max}) \approx \tau^{-3/4} \approx 0.031$, i.e. roughly 4 times slower than the normal speed. These estimates are for $j = 1$, i.e. fully recovered medium; in case of $j < 1$, e.g. in a re-entrant arrhythmia where waves closely follow one another, these safety margins drop down correspondingly, so the propagation block by front dissipation becomes increasingly feasible.

When a quantitative description is required, a less simplified model (12,13) can be used instead. The travelling front solutions may then need to be studied numerically, with a possible exception of qualitative questions like boundedness of the speed spectrum. We expect that the main features displayed by (15) will be preserved in such more accurate models, but this question needs further investigation.

Another direction for future study is development of the full singular perturbation theory for cardiac excitation propagation, similar to the classical theory developed for the FHN-type system, e.g. (Tyson & Keener 1988). In such theory, (12,13) would play the role of the fast subsystem, which needs to be supplemented by the slow subsystem, that would describe the evolution of the tissue outside the front, together with matching conditions. In such theory, the simplified model (14) or (15) can play the same role as Zel'dovich & Frank-Kamenetsky (1938) and (McKean 1970) solutions play for the asymptotic theory of FHN-type systems (Casten et al. 1975, Fife 1976, Tyson & Keener 1988), i.e. simple example admitting exact solutions, allowing simple test of the results of the general theory. One challenge for this asymptotic theory-to-be is the case of more than one spatial dimension. In the classical FHN-type theory, the fronts and backs, at any given moment of time, are located near lines separating two regions, excited region where $E(x, t) \approx E_+(v(x, t))$ and recovering region where $E(x, t) \approx E_-(v(x, t))$. So, e.g. in two spatial dimensions, the fronts and backs always form closed curves or curves ending on the medium boundaries, since $E_-(v)$ and $E_+(v)$ for the considered class of systems are well separated from each other, and their connection in space is by definition a front or a back. It is not so in the realistic models, since an excited and a recovering regions can be connected without forming a front between them (which happens e.g.

after a front has dissipated), and the back as such is not a well defined object. Thus, the fronts would be represented by lines which are not necessarily closed or ending on medium boundaries, but may end within the medium. These free front ends may result from localised propagation blocks (wavebreaks) and serve as tips of the spiral waves. Under certain technical conditions, the dynamics of such tips may be amenable to the asymptotic theory developed earlier for generic non-FHN type systems (Elkin, Biktashev & Holden 1998).

Acknowledgments

Author is grateful to I.V. Biktasheva for stimulating discussions and to V.V. Goryunov for the reference (Milnor 1963). This work was supported in parts by MRC and EPSRC.

References

- Aliev, R. R., Baudenbacher, F., Baudenbacher, P. & Wikswo, J. P. (2002), ‘Spatio-temporal dynamics of damped propagation in the heart’, *Phys. Rev. Letters*. Submitted.
- Aliev, R. R. & Panfilov, A. V. (1996), ‘A simple two-variable model of cardiac excitation’, *Chaos Solitons & Fractals* **7**, 293–301.
- Bernus, O., Wilders, R., Zemlin, C. W., Verschelde, H. & Panfilov, A. V. (2002), ‘A computationally efficient electrophysiological model of human ventricular cells’, *Am. J. Physiol.* **282**, H2296–H2308.
- Casten, R. G., Cohen, H. & Lagerstrom, P. A. (1975), ‘Perturbation analysis of an approximation to the Hodgkin-Huxley theory’, *Quart. Appl. Math.* **32**, 365–402.
- Courtemanche, M., Ramirez, R, J. & Nattel, S. (1998), ‘Ionic mechanisms underlying human atrial action potential properties: insights from a mathematical model’, *Am. J. Physiol.* **275**, H301–H321.
- Duckett, G. & Barkley, D. (2000), ‘Modeling the dynamics of cardiac action potentials’, *Phys. Rev. Lett.* **85**, 884–887.
- Elkin, Y. E., Biktashev, V. N. & Holden, A. V. (1998), ‘On the movement of excitation wave breaks’, *Chaos Solitons & Fractals* **9**, 1597–1610.
- Fenton, F. & Karma, A. (1998), ‘Vortex dynamics in three-dimensional continuous myocardium with fiber rotation: Filament instability and fibrillation’, *Chaos* **8**, 20–47.
- Fife, P. C. (1976), ‘Pattern formation in reacting and diffusing systems’, *J. Chem. Phys.* **64**, 554–564.
- FitzHugh, R. A. (1961), ‘Impulses and physiological states in theoretical models of nerve membrane’, *Biophys. J.* **1**, 445–466.
- Hinch, R. (2002), ‘An analytical study of the physiology and pathology of the propagation of cardiac action potentials’, *Progress in Biophysics and Molecular Biology* **78**, 45–81.
- Hodgkin, A. L. & Huxley, A. F. (1952), ‘A quantitative description of membrane current and its application to conduction and excitation in nerve’, *J. Physiol.* **117**, 500–544.
- Kagiyama, Y., Hill, J. L. & Gettes, L. S. (1982), ‘Interaction of acidosis and increased extracellular potassium on action potential characteristics and conduction in guinea pig ventricular muscle’, *Circ. Res.* **51**, 614–623.

- Krinsky, V. I. & Kokoz, Y. M. (1973), ‘Analysis of equations of excitable membranes — I. Reduction of the Hodgkin-Huxley equations to a second order system’, *Biofizika* **18**, 506–511.
- McKean, Jr., H. P. (1970), ‘Nagumo’s equation’, *Adv. Math.* **4**, 209–223.
- Milnor, J. (1963), *Morse Theory*, number 51 in ‘Annals of Mathematical Studies’, Princeton University Press, Princeton, New Jersey.
- Murray, J. (1989), *Mathematical Biology*, Springer Verlag, Berlin and others. See Chapter 11.5.
- Nagumo, J., Arimoto, S. & Yoshizawa, S. (1962), ‘An active pulse transmission line simulating nerve axon’, *Proc. IRE* **50**, 2061–2070.
- Rinzel, J. & Terman, D. (1982), ‘Propagation phenomena in a bistable reaction-diffusion system’, *SIAM J. Appl. Math.* **42**(5), 1111–1137.
- Suckley, R. & Biktashev, V. N. (2003), ‘Asymptotic structure of the Hodgkin-Huxley equations’, *Int. J. of Bifurcation and Chaos*. Submitted (in this issue).
- Tyson, J. J. & Keener, J. P. (1988), ‘Singular perturbation theory of traveling waves in excitable media (a review)’, *Physica D* **32**, 327–361.
- Weiss, J. N., Chen, P.-S., Qu, Z., Karagueuzian, H. S. & Garfinkel, A. (2000), ‘Ventricular fibrillation : How do we stop the waves from breaking?’, *Circ. Res.* **87**, 1103–1107.
- Zeeman, E. C. (1972), *Differential Equations For The Heartbeat And Nerve Impulse*, Mathematics Institute, University Of Warwick, Coventry.
- Zel’dovich, Y. B. & Frank-Kamenetsky, D. A. (1938), ‘Towards the theory of uniformly propagating flames’, *Doklady AN SSSR* **19**, 693–697.